International School and Workshop on Electronic Crystals, ECRYS 2022
Cargese, Corsica, France
August 18, 2022

Oscillating charge order and spin polarization in photoexcited Mott insulators

Kenji Yonemitsu

Dept. of Physics, Chuo Univ.

Collaboration with: N. Arakawa, T. Shimada (Chuo Univ.), P. Werner (Univ. of Fribourg),
T. Amano, Y. Kawakami, H. Itoh, K. Ohgushi, T. Sasaki, S. Iwai (Tohoku Univ.),
Y. Nakamura, H. Kishida (Nagoya Univ.), H. M. Yamamoto (IMS), K. Yamamoto (Okayama Univ. Sci.)

Supported by JSPS KAKENHI Grant Number JP16K05459,
MEXT Q-LEAP Grant Number JPMXS0118067426,
JST CREST Grant Number JPMJCR1901, Japan

Manipulation of many-electron states by light

- Ultrafast
- Far from equilibrium
- Symmetry different from equilibrium one
- Transient order
  - Synchronized charge motion after pulse: 1st topic
  - Effective magnetic fields during photoex.: 2nd topic

Organic dimer-Mott/SC: κ-(ET)$_2$X

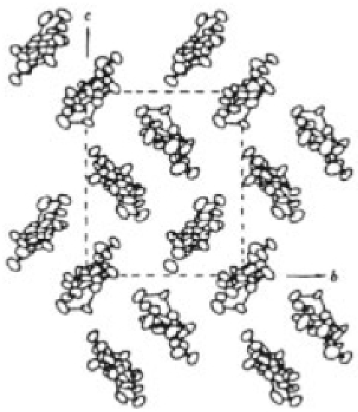

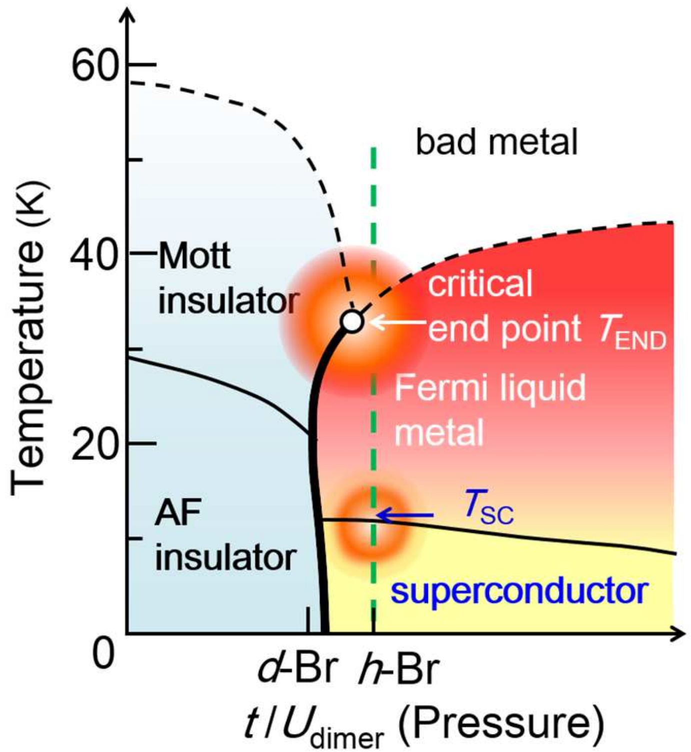

- Metal-Mott-insulator transition
- SC, AF, SL, criticality, etc.
- Molecular DOF in dimers
  - Anomalous dielectric permittivity
  - Photoinduced IM trans. – bandwidth/filling
  - Stimulated emission at a high energy

Y. Kawakami, S. Iwai et al., *PRL* **103**, 066403 (2009).

Y. Kawakami, KY, S. Iwai et al., *Nat. Photon.* **12**, 474 (2018).

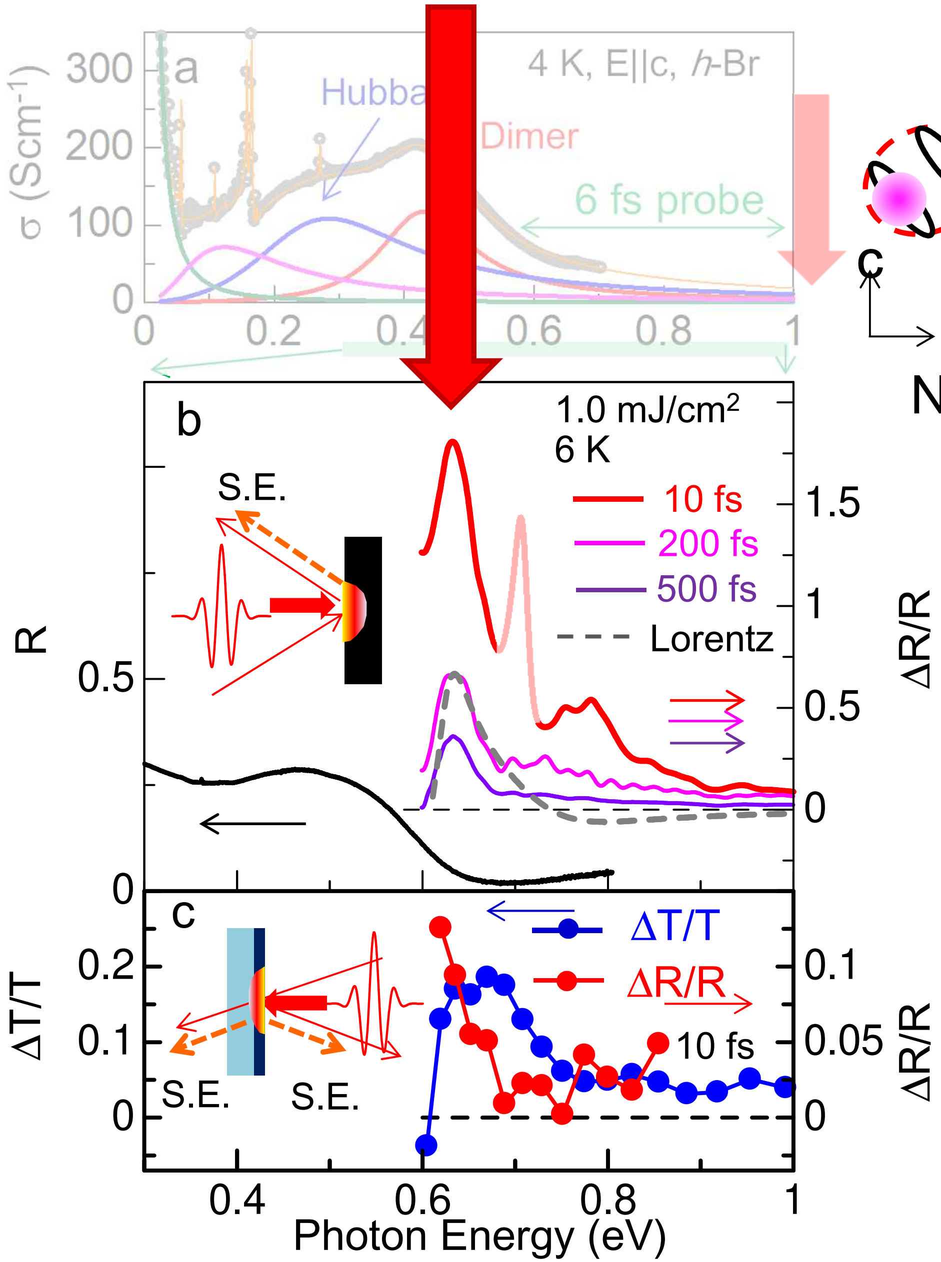

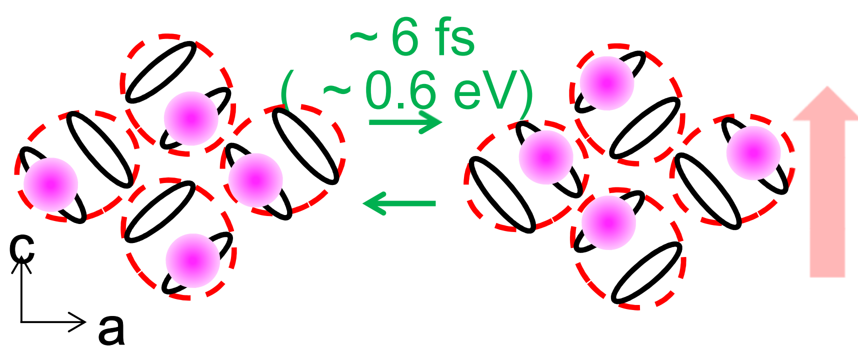

Non-linear charge oscillation

Stimulated emission is observed in κ-(BEDT-TTF)$_2$Cu[N(CN)$_2$]Br only after a strong pulse: similarity to a negative-temperature state

Y. Kawakami et al., *Nat. Photonics* **12**, 474 (2018).

2D 3/4-filled Hubbard model for κ-(ET)$_2$X

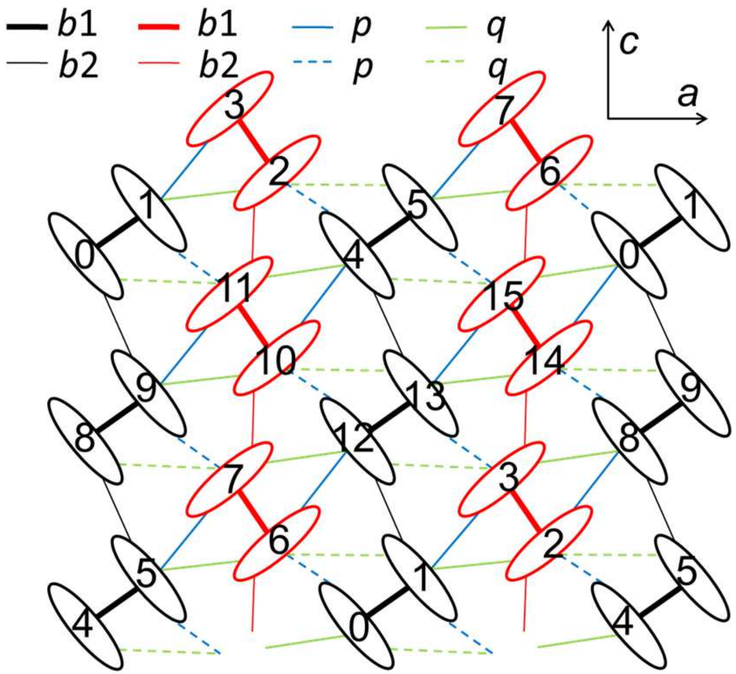

$$H = \sum_{\langle i,j\rangle\sigma} t_{ij}\left(c_{i,\sigma}^{\dagger} c_{j,\sigma} + c_{j,\sigma}^{\dagger} c_{i,\sigma}\right) + U \sum_{i} n_{i\uparrow} n_{i\downarrow}$$

Exact diagonalization

Photoexcitation

$$c_{i,\sigma}^{+} c_{j,\sigma} \rightarrow \exp\left[\frac{ie}{\hbar c}\mathbf{r}_{ij} \cdot \mathbf{A}(t)\right] c_{i,\sigma}^{+} c_{j,\sigma}$$

where $\boldsymbol{r}_{ij} = \boldsymbol{r}_j - \boldsymbol{r}_i$,
substituted into Hamiltonian H

1-cycle pulse

$$\boldsymbol{A}(t) = \frac{c\boldsymbol{F}}{\omega}[\cos(\omega t) - 1]\theta(t)\theta\left(\frac{2\pi}{\omega} - t\right)$$

$\boldsymbol{F}$ // a or c

Time evolution

time-dependent Schrödinger eq.

$$i\hbar \frac{\partial}{\partial t}\Psi = H\{A(t)\}\Psi$$

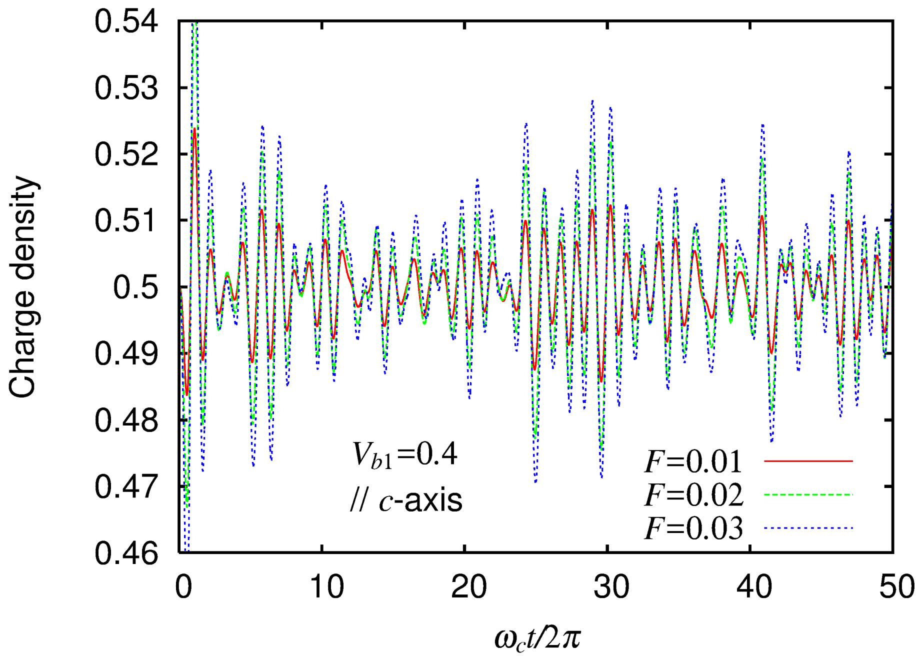

Time profile of charge density at i=0

$$\left(2-\sum_{\sigma}\left\langle c_{i,\sigma}^{+}c_{i,\sigma}\right\rangle\right)$$

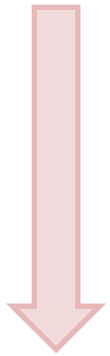

Fourier transform
after photoexcitation

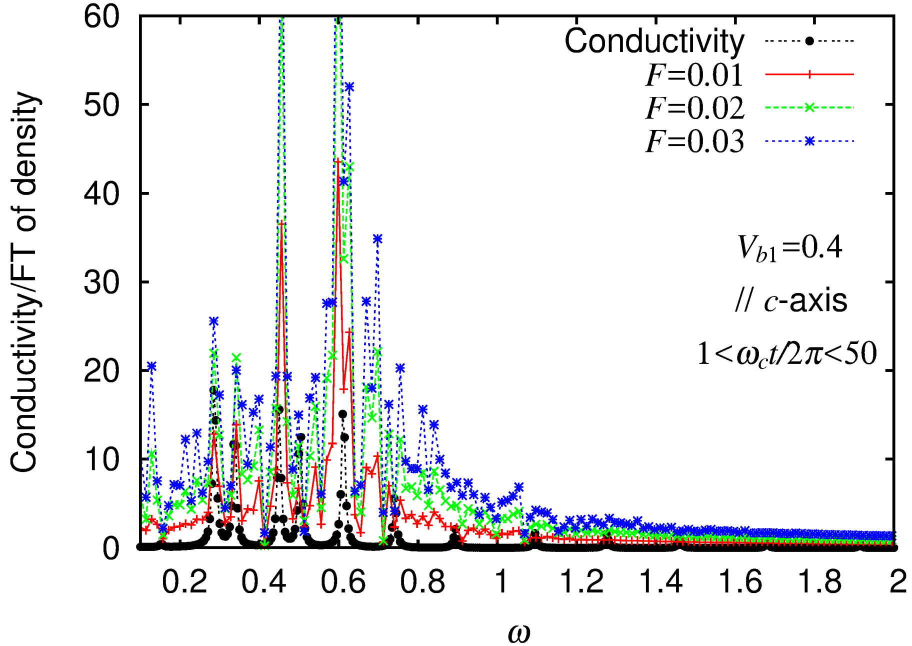

For small F,
FT of charge-density time profile shows peaks at energies where $\sigma(\omega)$ has peaks.

KY, *JPSJ* **87**, 044708 (2018).

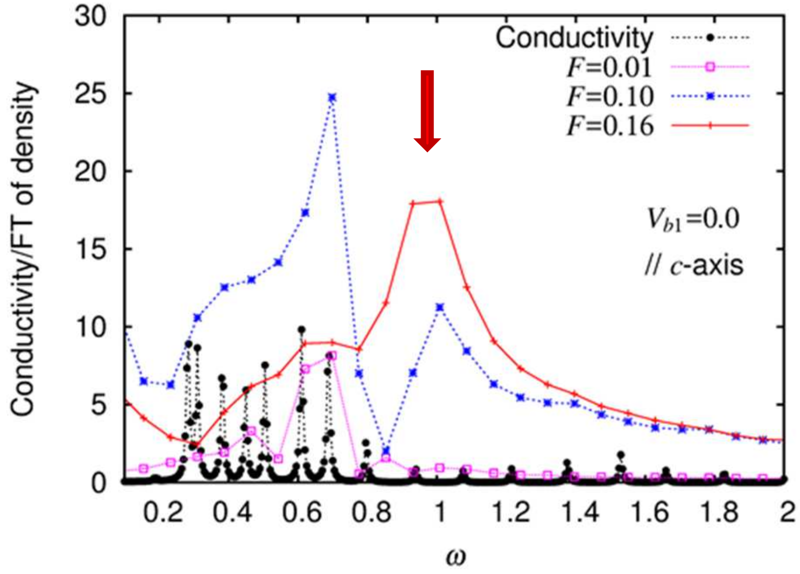

For large *F*,
FT of charge-density time profile shows a peak at $\omega_{\rm osc}$ on the high-energy side of $\sigma(\omega)$.

$$\omega_{\rm osc} = 2\left(|t_{b1}| + |t_{b2}| + 2|t_q|\right)$$

KY, *JPSJ* **87**, 044708 (2018).

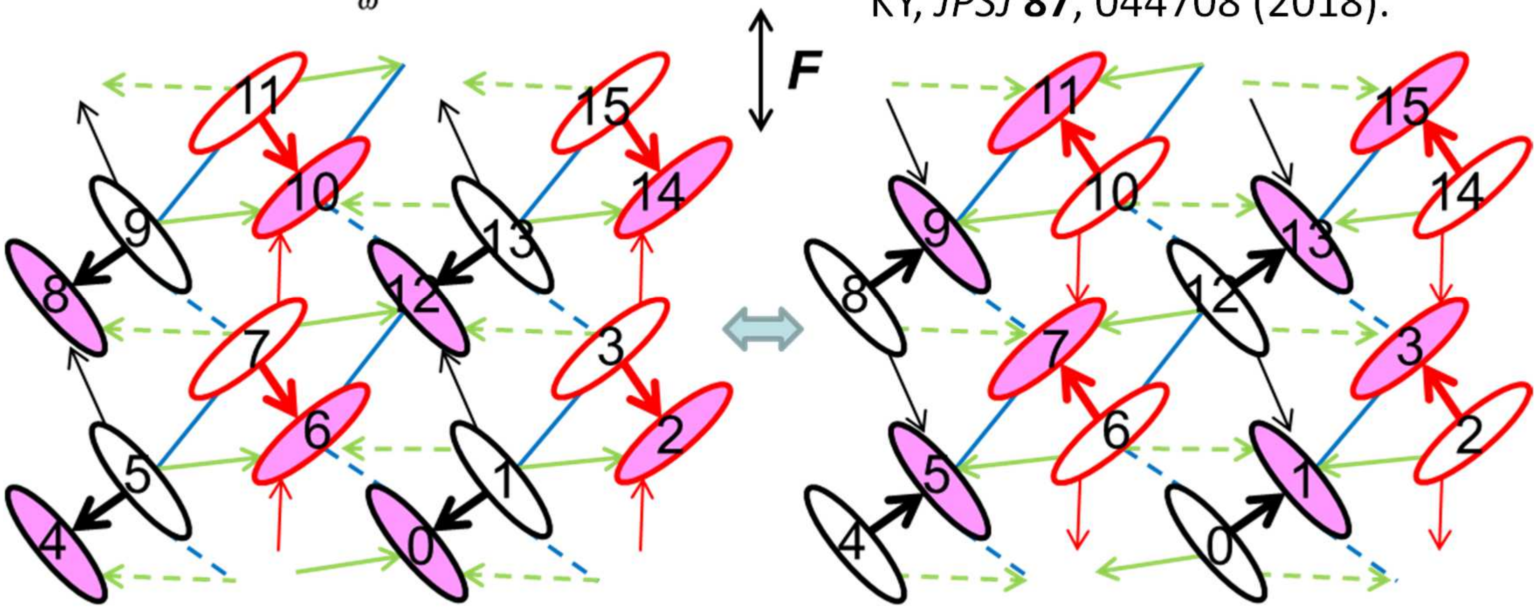

Single frequency in spite of different $|t|$ and $\boldsymbol{r}_{ij}$ → Synchronization?

To investigate whether synchronization occurs

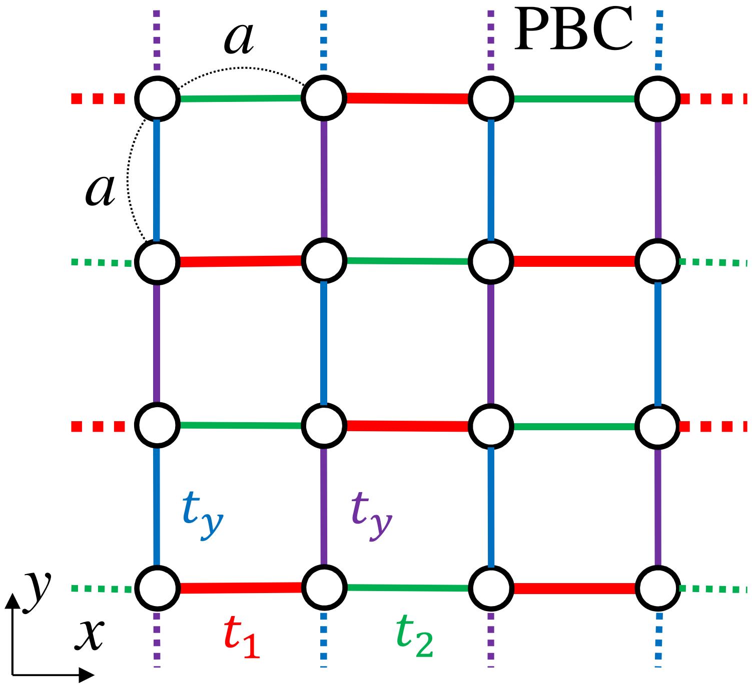

$t_1 = -0.3$, $t_2 = -0.1$, $t_y = -0.1$ & random numbers

$$H = \sum_{\langle i,j\rangle\sigma} t_{ij}\left(c^\dagger_{i,\sigma}c_{j,\sigma} + c^\dagger_{j,\sigma}c_{i,\sigma}\right) + U\sum_i n_{i\uparrow}n_{i\downarrow}$$

at 3/4 filling

Random numbers added on every bond:

$$\boldsymbol{t_{ij}} \to \boldsymbol{t_{ij}}\left(\boldsymbol{1} + \boldsymbol{\delta_{ij}}\right) \quad \text{where} \quad \boldsymbol{\delta_{ij}} \in [-\boldsymbol{\varepsilon}, \boldsymbol{\varepsilon}]$$

Synchronization order parameter: $\boldsymbol{r(t)}$

$$r(t)e^{i\psi(t)} = \frac{1}{M}\sum_{m=1}^{M} e^{i\phi_m(t)}$$

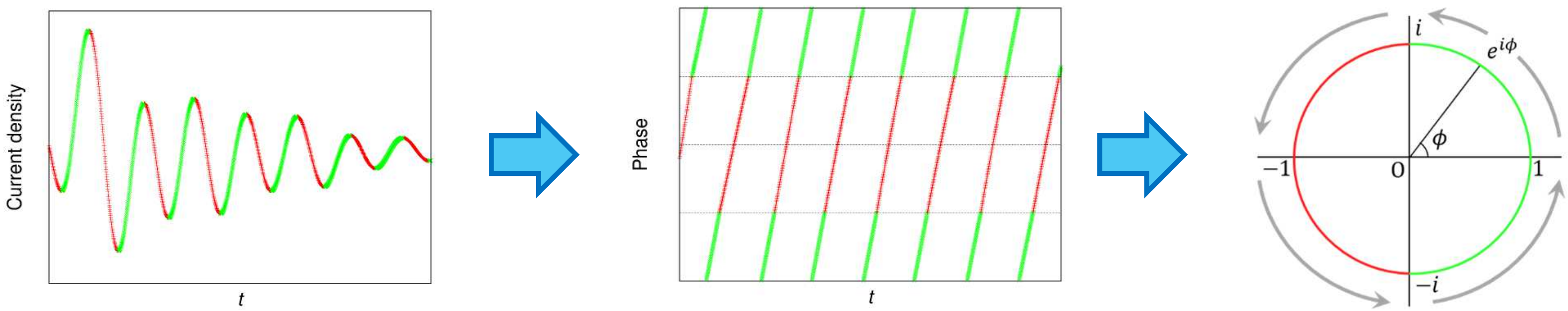

T. Shimada & KY, *JPSJ* **89**, 084701 (2020).

Synchronization order parameter

(average over $3T < t < 6T$ after excitation $0 < t < T$
& average over random number distributions)

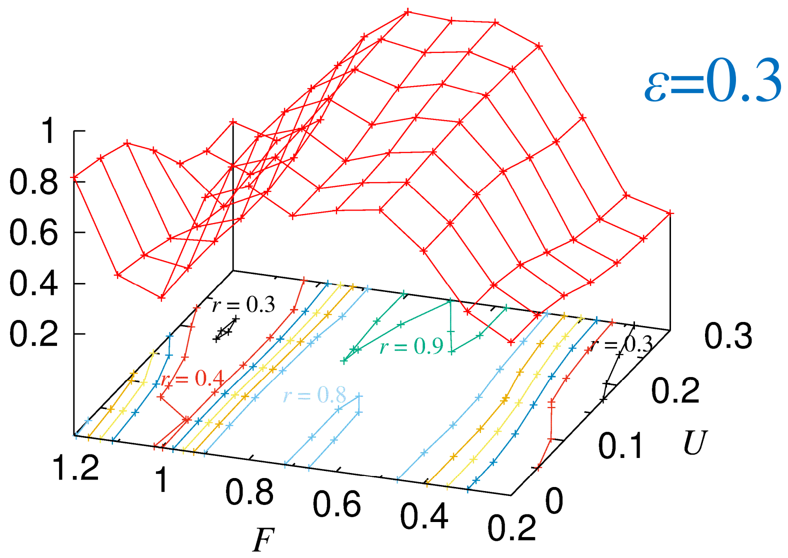

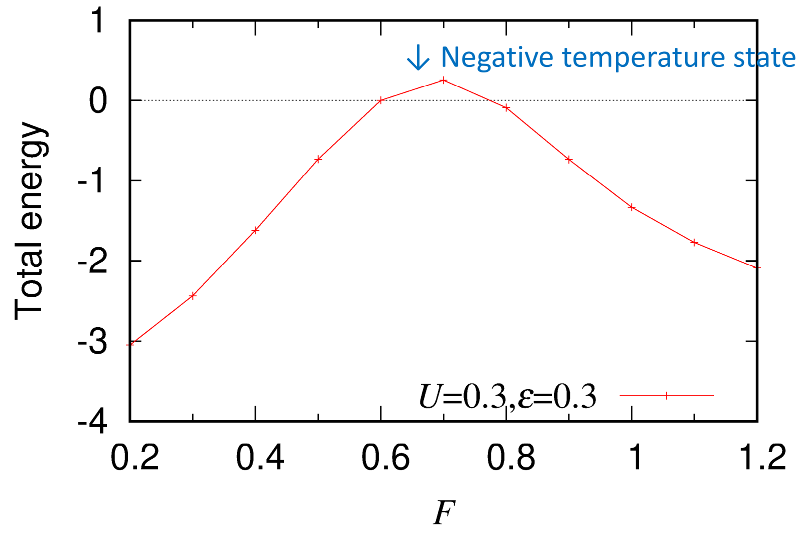

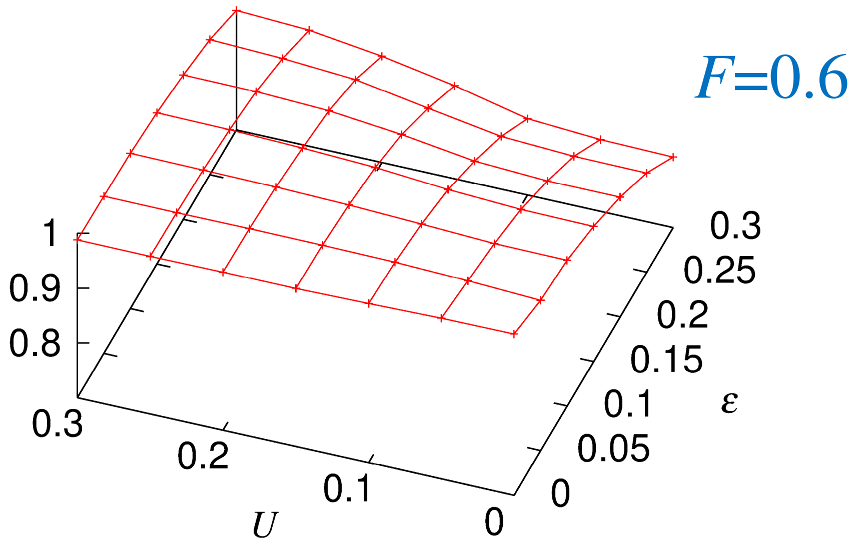

Randomness ε decreases the order parameter.

Competition

On-site repulsion U increases the order parameter.

T. Shimada & KY, *JPSJ* **89**, 084701 (2020).

To investigate how synchronization occurs

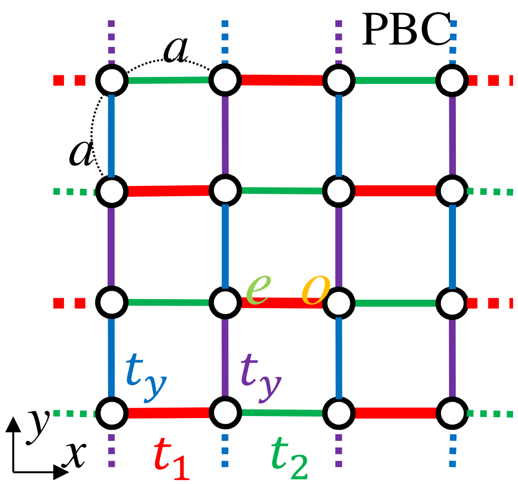

Generally, on a dimerized lattice

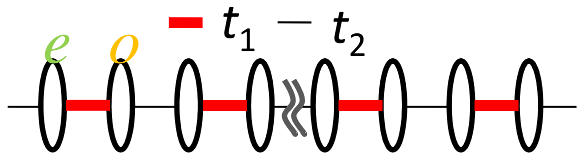

$$\begin{pmatrix} e_{\boldsymbol{k}\sigma}^\dagger & o_{\boldsymbol{k}\sigma}^\dagger \end{pmatrix} = \begin{pmatrix} e_{\boldsymbol{k}\sigma}'^\dagger & o_{\boldsymbol{k}\sigma}'^\dagger \end{pmatrix} \begin{pmatrix} e^{-i\frac{\phi_{\boldsymbol{k}}}{2}} & 0 \\ 0 & e^{i\frac{\phi_{\boldsymbol{k}}}{2}} \end{pmatrix}$$

$$H_{\mathrm{MF}} = \sum_{\boldsymbol{k}\sigma} \begin{pmatrix} e_{\boldsymbol{k}\sigma}^\dagger & o_{\boldsymbol{k}\sigma}^\dagger \end{pmatrix} \begin{pmatrix} \frac{U}{2}\delta n & h(\boldsymbol{k}) \\ h^*(\boldsymbol{k}) & -\frac{U}{2}\delta n \end{pmatrix} \begin{pmatrix} e_{\boldsymbol{k}\sigma} \\ o_{\boldsymbol{k}\sigma} \end{pmatrix}$$

$$\begin{pmatrix} e_{\boldsymbol{k}\sigma}'^\dagger & o_{\boldsymbol{k}\sigma}'^\dagger \end{pmatrix} = \begin{pmatrix} a_{\boldsymbol{k}\sigma}^\dagger & b_{\boldsymbol{k}\sigma}^\dagger \end{pmatrix} \frac{1}{\sqrt{2}} \begin{pmatrix} 1 & -1 \\ 1 & 1 \end{pmatrix}$$

$$H_{\mathrm{MF}} = \sum_{\boldsymbol{k}\sigma} \begin{pmatrix} a_{\boldsymbol{k}\sigma}^\dagger & b_{\boldsymbol{k}\sigma}^\dagger \end{pmatrix} \begin{pmatrix} -h'(\boldsymbol{k}) & \frac{U}{2}\delta n \\ \frac{U}{2}\delta n & h'(\boldsymbol{k}) \end{pmatrix} \begin{pmatrix} a_{\boldsymbol{k}\sigma} \\ b_{\boldsymbol{k}\sigma} \end{pmatrix}$$

(antibonding & bonding)

$$\delta n = \langle e_{i\sigma}^\dagger e_{i\sigma} - o_{i\sigma}^\dagger o_{i\sigma} \rangle = \frac{1}{N}\sum_{\boldsymbol{k}} \langle e_{\boldsymbol{k}\sigma}^\dagger e_{\boldsymbol{k}\sigma} - o_{\boldsymbol{k}\sigma}^\dagger o_{\boldsymbol{k}\sigma} \rangle = \frac{1}{2N}\sum_{\boldsymbol{k}\sigma} \langle a_{\boldsymbol{k}\sigma}^\dagger b_{\boldsymbol{k}\sigma} + b_{\boldsymbol{k}\sigma}^\dagger a_{\boldsymbol{k}\sigma} \rangle$$

$$r_{1\boldsymbol{k}\sigma} = \langle a_{\boldsymbol{k}\sigma}^\dagger b_{\boldsymbol{k}\sigma} + b_{\boldsymbol{k}\sigma}^\dagger a_{\boldsymbol{k}\sigma} \rangle$$

$$r_{2\boldsymbol{k}\sigma} = \langle -i a_{\boldsymbol{k}\sigma}^\dagger b_{\boldsymbol{k}\sigma} + i b_{\boldsymbol{k}\sigma}^\dagger a_{\boldsymbol{k}\sigma} \rangle$$

$$r_{3\boldsymbol{k}\sigma} = \langle a_{\boldsymbol{k}\sigma}^\dagger a_{\boldsymbol{k}\sigma} - b_{\boldsymbol{k}\sigma}^\dagger b_{\boldsymbol{k}\sigma} \rangle$$

$r_{1k\sigma}$: Density difference between e&o sublattices

$r_{2k\sigma}$: Current density between e&o sublattices

$r_{3k\sigma}$: Bond density between e&o sublattices

Bloch equations for Larmor precession under "magnetic" field

$$\dot{r}_{1\boldsymbol{k}\sigma} = 2h'(\boldsymbol{k})\, r_{2\boldsymbol{k}\sigma}$$
$$\dot{r}_{2\boldsymbol{k}\sigma} = -2h'(\boldsymbol{k})\, r_{1\boldsymbol{k}\sigma} - 2\Omega r_{3\boldsymbol{k}\sigma}$$
$$\dot{r}_{3\boldsymbol{k}\sigma} = 2\Omega\, r_{2\boldsymbol{k}\sigma}$$

$$\Omega \equiv \frac{U}{2}\delta n = \frac{U}{4N}\sum_{\boldsymbol{k}\sigma} r_{1\boldsymbol{k}\sigma}$$

Static $\delta n \neq 0$ solution is absent for $U > 0$.

$$\dot{\boldsymbol{r}}_{\boldsymbol{k}\sigma}(t) = \boldsymbol{B}_{\boldsymbol{k}}(t) \times \boldsymbol{r}_{\boldsymbol{k}\sigma}(t)$$
$$\boldsymbol{B}_{\boldsymbol{k}}(t) = (B_{1\boldsymbol{k}}(t), B_{2\boldsymbol{k}}, B_{3\boldsymbol{k}}) = (2\Omega(t) = U\delta n(t), 0, -2h'(\boldsymbol{k}) > 0)$$

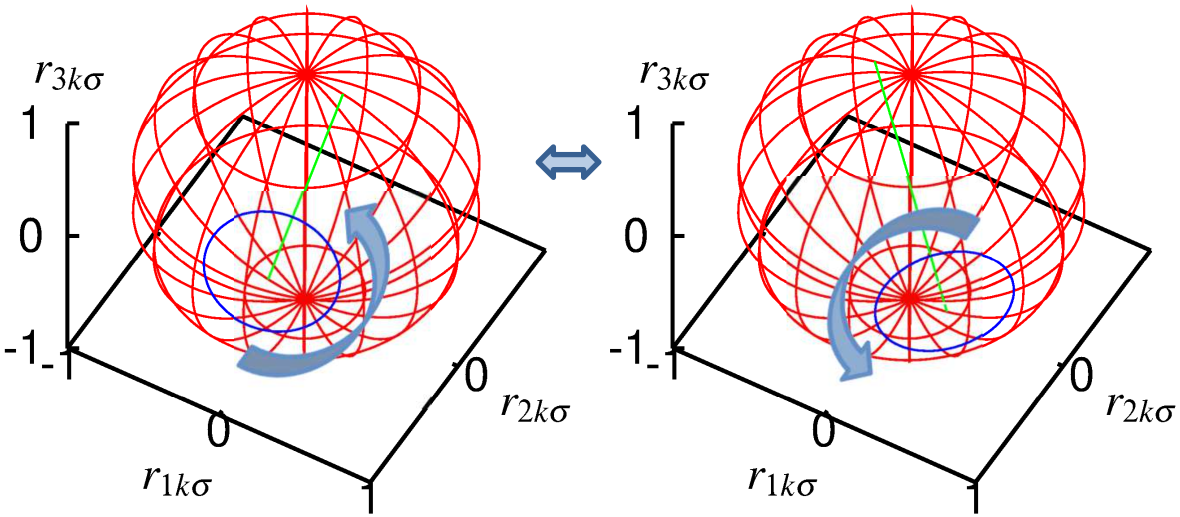

$r_{1k\sigma}$: Density difference $r_{2k\sigma}$: Current density $r_{3k\sigma}$: Bond density

$U > 0$ and $V < 0$ enhance the current flow, both in k-space and in r-space.

KY & P. Werner, *JPSJ* **90**, 044713 (2021).

Dynamics in Hubbard model on 1D dimerized lattice

Near-equilibrium vs. far-from-equilibrium:
Linear charge oscillations vs. electronic breathing mode
thru sync. at $\omega_{\mathrm{osc}} = 2\sum|t_{eo}| = 0.8$

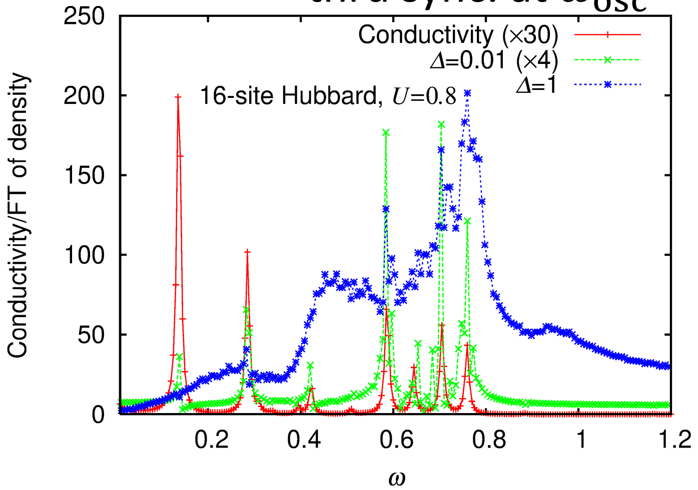

Far-from-equilibrium:
Independence from the initial condition

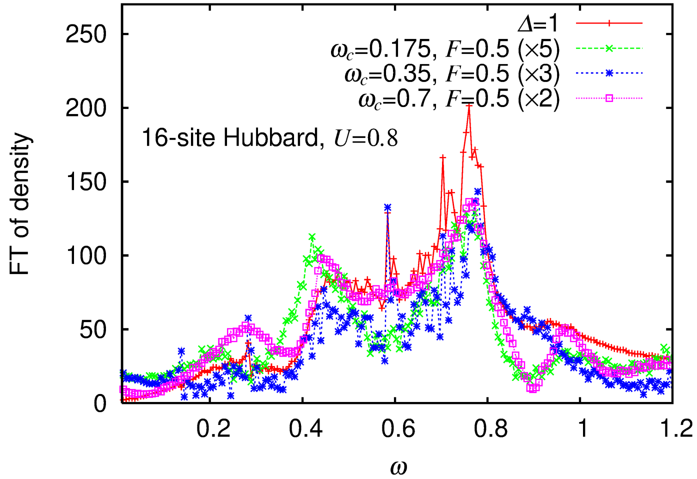

System-size dependence: small *U* and large *U* limits = integrable; no synchronization

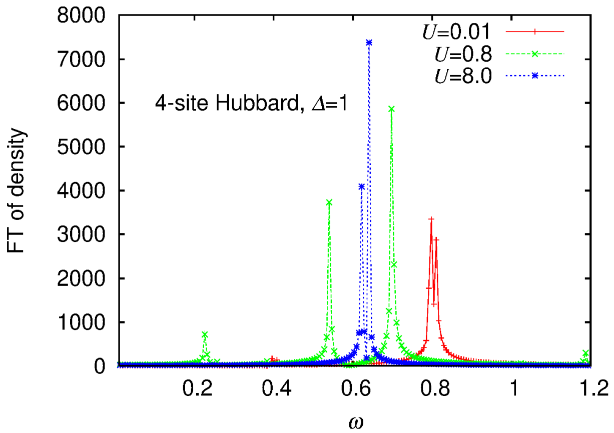

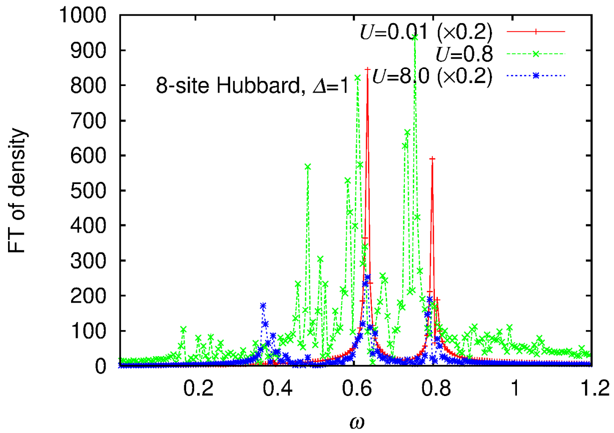

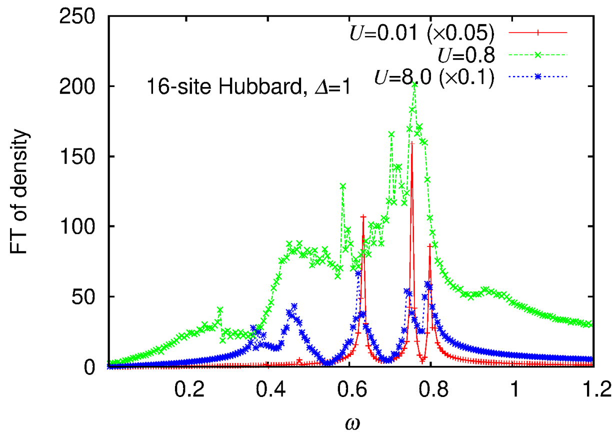

KY & P. Werner, *JPSJ* **90**, 044713 (2021).

Summary on synch. charge motion in dimer lattices

- Charge oscillation after strong pulse excitation.
- Synchronization even with different transfer integrals (with random numbers added to).
- On-site repulsion *U* gives bond-independent force that enhances current flow.
  - Rotation axis in Bloch equation tilts into the opposite direction from that for SC, CDW, etc.

Quantum spin-liquid system: α-RuCl$_3$

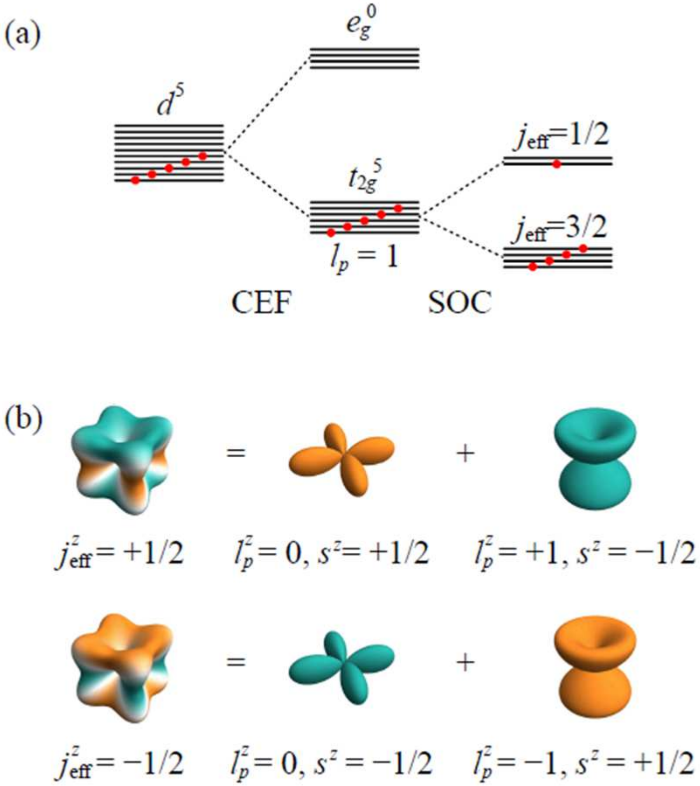

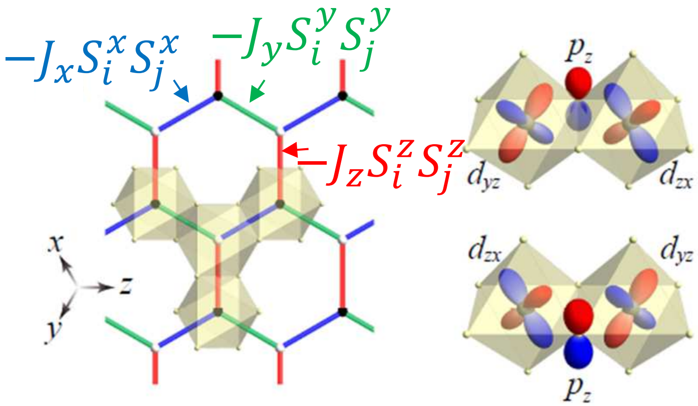

Y. Motome and J. Nasu, JPSJ 2020

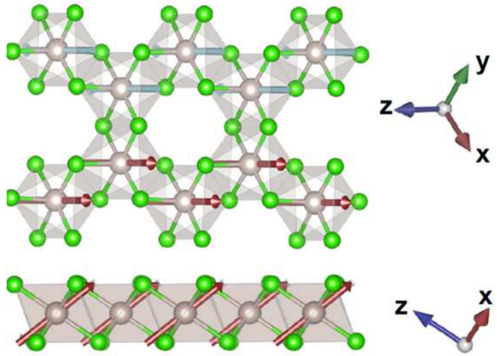

S. M. Winter et al., PRB 2016

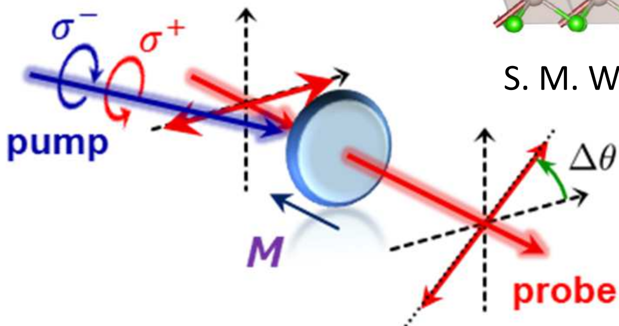

T. Amano, KY, S. Iwai *et al.*, PRR 2022

- Theories
  - A. Kitaev, Ann. Phys. 321, 2 (2006)
  - G. Jackeli and G. Khaliullin, PRL 102, 017205 (2009)
  - H.-S. Kim and H.-Y. Kee, PRB 93, 155143 (2016).
  - S. M. Winter *et al.*, PRB 93, 214431 (2016).
- Experiments
  - L. J. Sandilands *et al.*, PRB 93, 075144 (2016).
  - L. J. Sandilands *et al.*, PRB 94, 195156 (2016).
  - P. Warzanowski *et al.*, PRR 2, 042007(R) (2020).

Three-orbital Hubbard model for Kitaev materials

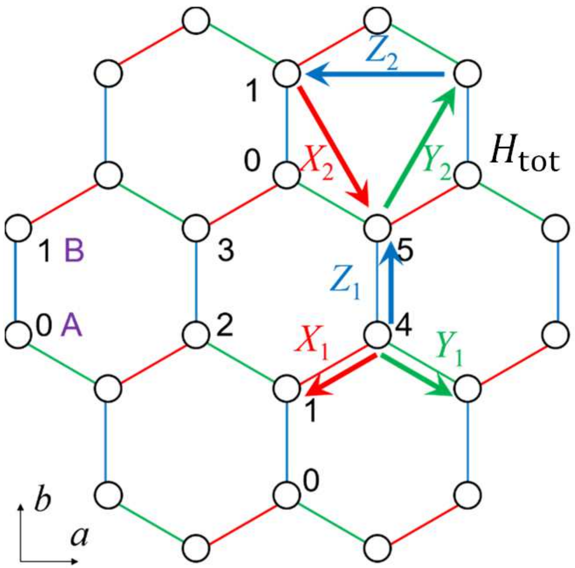

p.b.c., 6 sites (3 unit cells)

S. M. Winter, Y. Li, H. O. Jeschke, and Roser Valentí, PRB2016

$$H_{\rm tot} = H_{\rm hop} + H_{\rm CF} + H_{\rm SO} + H_U$$

$$\vec{c}_i^\dagger = \left(c_{i,yz,\uparrow}^\dagger\ c_{i,yz,\downarrow}^\dagger\ c_{i,xz,\uparrow}^\dagger\ c_{i,xz,\downarrow}^\dagger\ c_{i,xy,\uparrow}^\dagger\ c_{i,xy,\downarrow}^\dagger\right)$$

(hole picture)

$$H_{\rm hop} = -\sum_{ij} \vec{c}_i^\dagger \{\mathbf{T}_{ij} \otimes \mathbb{I}_{2\times 2}\} \vec{c}_j$$

$$\mathbf{T}_1^{\rm X} = \begin{pmatrix} t_3 & t_4 & t_4 \\ t_4 & t_1 & t_2 \\ t_4 & t_2 & t_1 \end{pmatrix} \quad \mathbf{T}_1^{\rm Y} = \begin{pmatrix} t_1 & t_4 & t_2 \\ t_4 & t_3 & t_4 \\ t_2 & t_4 & t_1 \end{pmatrix} \quad \mathbf{T}_1^{\rm Z} = \begin{pmatrix} t_1 & t_2 & t_4 \\ t_2 & t_1 & t_4 \\ t_4 & t_4 & t_3 \end{pmatrix}$$

$$H_{\rm SO} = \frac{\lambda}{2} \sum_i \vec{c}_i^\dagger \begin{pmatrix} 0 & -i\sigma_z & i\sigma_y \\ i\sigma_z & 0 & -i\sigma_x \\ -i\sigma_y & i\sigma_x & 0 \end{pmatrix} \vec{c}_i$$

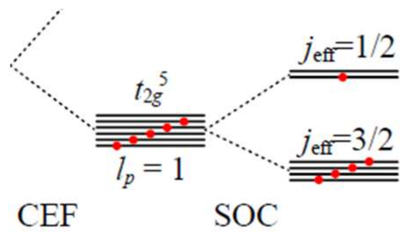

Y. Motome and J. Nasu, JPSJ 2020

$H_U = U, U', J_{\rm H}$ terms $\quad U' = U - 2J_{\rm H}$

$J_{\rm eff} = \frac{1}{2}$: half filled

$$\left|\frac{1}{2}, \frac{1}{2}\right\rangle = p_\uparrow^\dagger |0\rangle \equiv \frac{1}{\sqrt{3}}\left(-c_{xy,\uparrow}^\dagger - i c_{xz,\downarrow}^\dagger - c_{yz,\downarrow}^\dagger\right)|0\rangle$$

$$\left|\frac{1}{2}, -\frac{1}{2}\right\rangle = p_\downarrow^\dagger |0\rangle \equiv \frac{1}{\sqrt{3}}\left(c_{xy,\downarrow}^\dagger + i c_{xz,\uparrow}^\dagger - c_{yz,\uparrow}^\dagger\right)|0\rangle$$

$$m_x^{(1/2)} \equiv \frac{1}{2}\langle p_\uparrow^\dagger p_\downarrow + p_\downarrow^\dagger p_\uparrow \rangle$$

$$m_y^{(1/2)} \equiv \frac{1}{2}\langle -i p_\uparrow^\dagger p_\downarrow + i p_\downarrow^\dagger p_\uparrow \rangle$$

$$m_z^{(1/2)} \equiv \frac{1}{2}\langle p_\uparrow^\dagger p_\uparrow - p_\downarrow^\dagger p_\downarrow \rangle$$

$$m_\perp^{(1/2)} \equiv \frac{1}{\sqrt{3}}\left(m_x^{(1/2)} + m_y^{(1/2)} + m_z^{(1/2)}\right)$$

"Spin-orbit assisted Mott insulator"

- Hopping induced mixing between $J_{\rm eff} = \frac{1}{2}$ and $J_{\rm eff} = \frac{3}{2}$ is suppressed by Coulomb interaction -> half-filled Mott insulator.
- Excitation of in-gap states -> charge dynamics.

Ground-state results: optical conductivity

$$c^\dagger_{i,a,\sigma}c_{j,b,\sigma} \rightarrow \exp\left[-\frac{ie}{\hbar c}\boldsymbol{r}_{ij}\cdot\boldsymbol{A}(t)\right]c^\dagger_{i,a,\sigma}c_{j,b,\sigma}$$

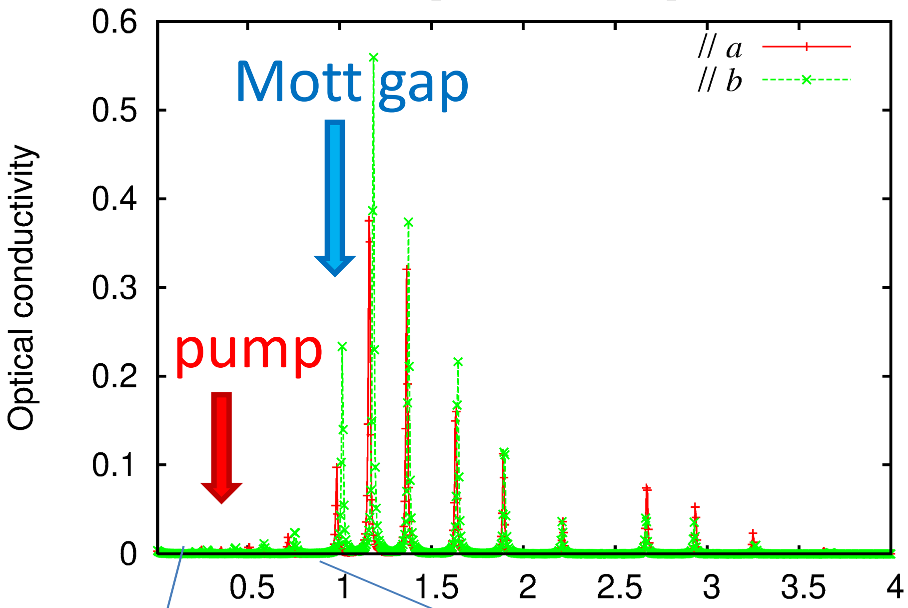

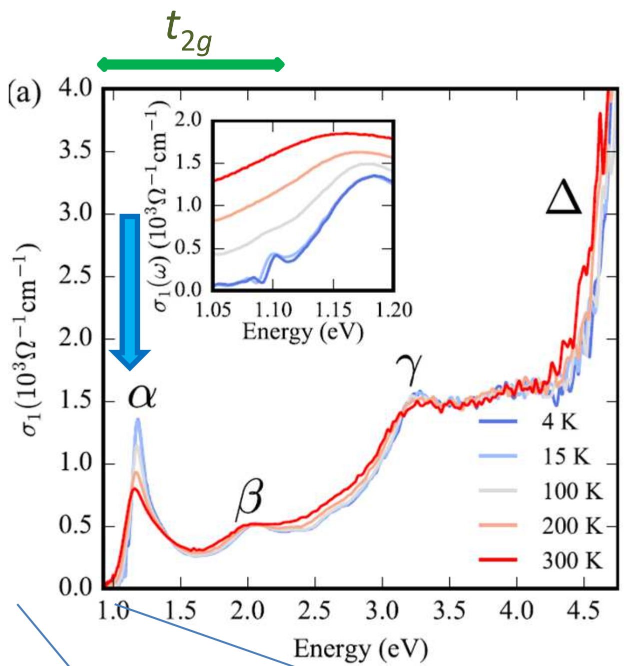

L. J. Sandilands et al., PRB 94, (2016)

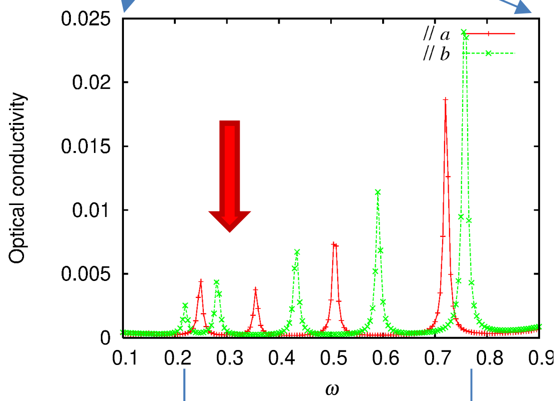

"Spin-orbit assisted Mott insulator"

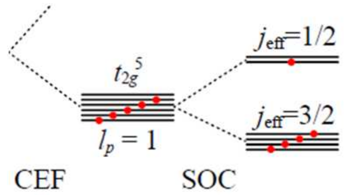

Y. Motome and J. Nasu, JPSJ 2020

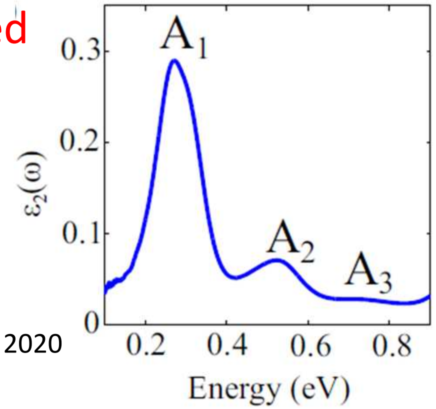

L. J. Sandilands et al., PRB 93, (2016)

Spin-orbit coupled in-gap states, "spin-orbit excitons," are excited by ω below the Mott gap.

P. Warzanowski et al., PRR 2, (2020)

Magnetization dynamics induced by circularly polarized light

Strong field case

$J^{1/2}_{x,y,z}$

$J^{3/2}_{x,y,z}$

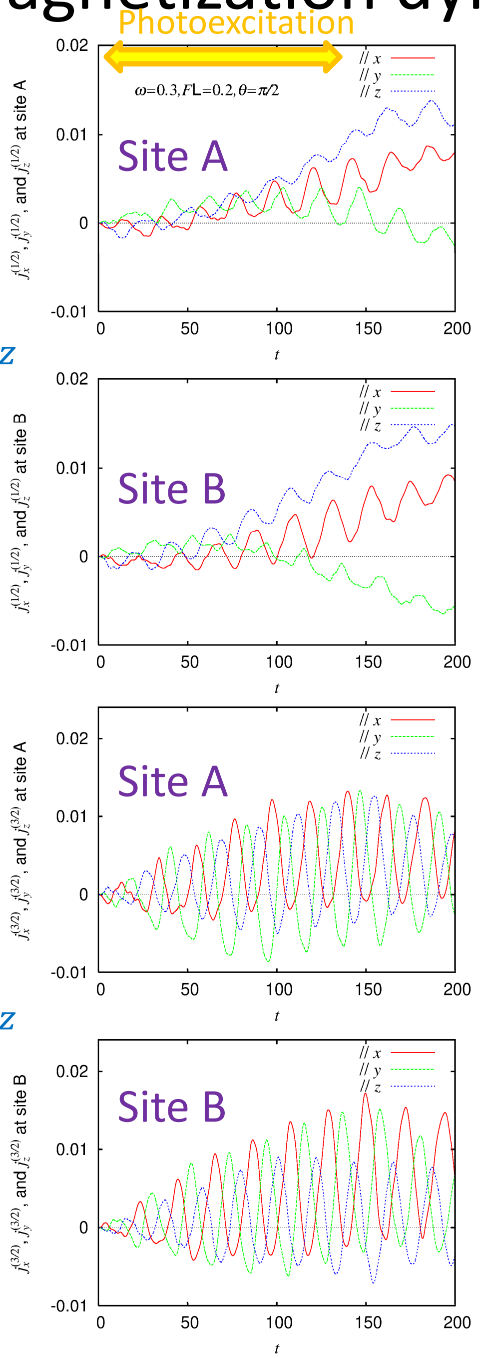

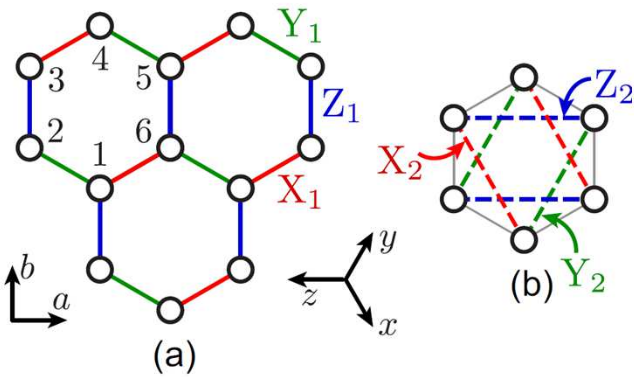

Quantum Floquet theory for periodically driven systems

$$H(t) = H(t+T)$$

The time-dependent Schrödinger equation,

$$i\hbar \frac{\partial}{\partial t} |\psi(t)\rangle = H(t)|\psi(t)\rangle \, ,$$

has a "stationary" solution,

$$|\psi_n(t)\rangle = |u_n(t)\rangle \, e^{-\frac{i}{\hbar}\varepsilon_n t} \, ,$$

ε_n: quasi-energy,

$|u_n(t)\rangle = |u_n(t+T)\rangle$: Floquet mode.

For stroboscopic evolution,

$$U(t_0+T, t_0)|\psi_n(t_0)\rangle = e^{-\frac{i}{\hbar}\varepsilon_n T}|\psi_n(t_0)\rangle \, ,$$

the Floquet Hamiltonian $H_{t_0}^{\mathrm{F}}$ defined as

$$U(t_0+T, t_0) = e^{-\frac{i}{\hbar}T H_{t_0}^{\mathrm{F}}} \quad \text{with} \quad H_{t_0}^{\mathrm{F}} = \sum_n \varepsilon_n |u_n(t_0)\rangle\langle u_n(t_0)|$$

can be obtained perturbatively, e.g., by a high-frequency expansion,

$$H_F = H_F^{(1)} \left[\equiv \frac{1}{T}\int_0^T dt H(t) \right] + H_F^{(2)} \left[\equiv \sum_{m>0} \frac{[H_m, H_{-m}]}{m\hbar\omega} \right] + \cdots$$

where

$$H_m = \frac{1}{T}\int_0^T dt e^{-im\omega t} H(t) \; .$$

Magnetization dynamics induced by circularly polarized light

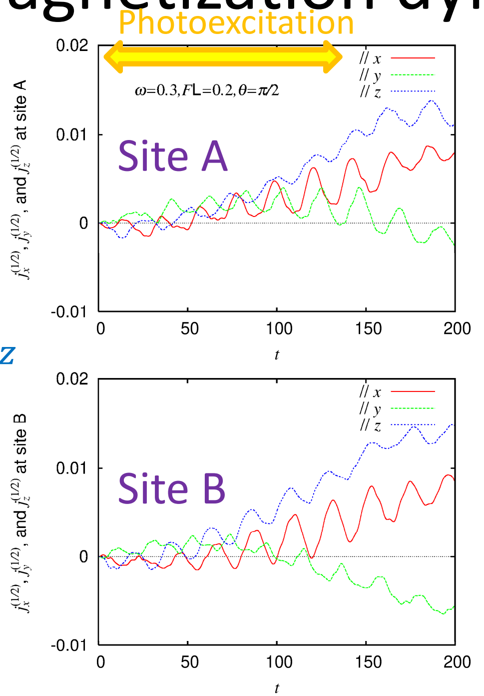

$J^{1/2}_{x,y,z}$

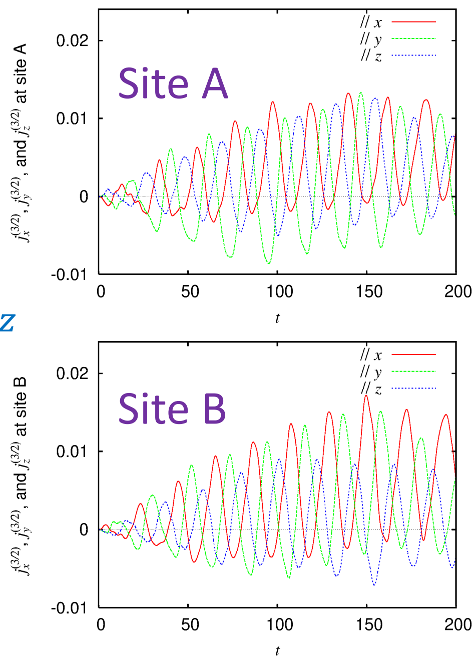

$J^{3/2}_{x,y,z}$

Strong field case

High-freq. expansion in Floquet theory: $H_F^{(2)}$

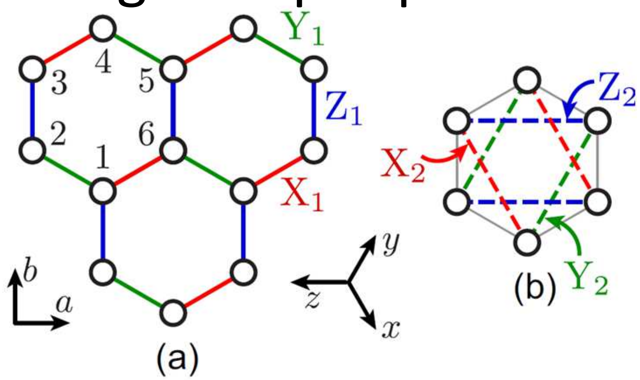

$$H_F^{(2)} = \sum_{m>0} \frac{[H_m, H_{-m}]}{m\hbar\omega}$$

For left-hand circular polarization and at site A,

$$H_F^{(2,A)} = \sum_{m>0} \frac{1}{m\hbar\omega} \sum_{\boldsymbol{k}ab\sigma} J_m^2\left(\frac{eaF_\mathrm{L}}{\hbar\omega}\right)(2i)\sin\frac{2m\pi}{3}(\star)_{ab}c^\dagger_{\boldsymbol{k},a,\sigma}c_{\boldsymbol{k},b,\sigma}$$

At site B, momenta are reversed.

where

$$\star = e^{i\boldsymbol{k}\cdot X_2}\mathrm{T}_1^\mathrm{Y}\mathrm{T}_1^\mathrm{Z} - e^{-i\boldsymbol{k}\cdot X_2}\mathrm{T}_1^\mathrm{Z}\mathrm{T}_1^\mathrm{Y} + e^{i\boldsymbol{k}\cdot Y_2}\mathrm{T}_1^\mathrm{Z}\mathrm{T}_1^\mathrm{X} - e^{-i\boldsymbol{k}\cdot Y_2}\mathrm{T}_1^\mathrm{X}\mathrm{T}_1^\mathrm{Z} + e^{i\boldsymbol{k}\cdot Z_2}\mathrm{T}_1^\mathrm{X}\mathrm{T}_1^\mathrm{Y} - e^{-i\boldsymbol{k}\cdot Z_2}\mathrm{T}_1^\mathrm{Y}\mathrm{T}_1^\mathrm{X}$$

$$= [\mathrm{T}_1^\mathrm{Y}, \mathrm{T}_1^\mathrm{Z}]\cos\boldsymbol{k}\cdot X_2 + [\mathrm{T}_1^\mathrm{Z}, \mathrm{T}_1^\mathrm{X}]\cos\boldsymbol{k}\cdot Y_2 + [\mathrm{T}_1^\mathrm{X}, \mathrm{T}_1^\mathrm{Y}]\cos\boldsymbol{k}\cdot Z_2$$

$$+ i\{\mathrm{T}_1^\mathrm{Y}, \mathrm{T}_1^\mathrm{Z}\}\sin\boldsymbol{k}\cdot X_2 + i\{\mathrm{T}_1^\mathrm{Z}, \mathrm{T}_1^\mathrm{X}\}\sin\boldsymbol{k}\cdot Y_2 + i\{\mathrm{T}_1^\mathrm{X}, \mathrm{T}_1^\mathrm{Y}\}\sin\boldsymbol{k}\cdot Z_2$$

- Single-orbital systems have only ***k***-odd terms with anticommutators.
- Multi-orbital systems have ***k***-even terms with commutators, in addition.

Magnetization dynamics induced by circularly polarized light

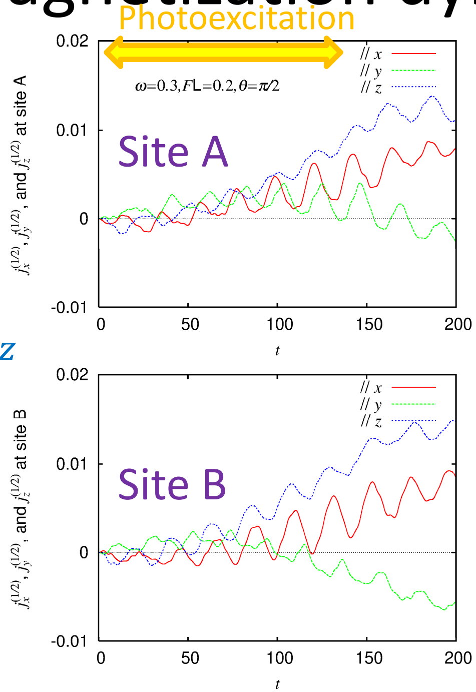

$J^{1/2}_{x,y,z}$

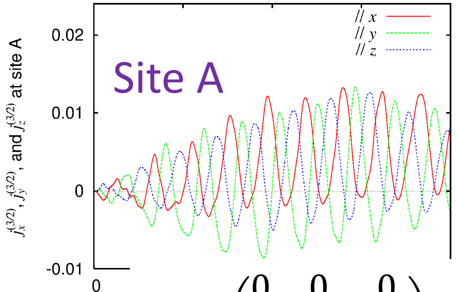

$J^{3/2}_{x,y,z}$

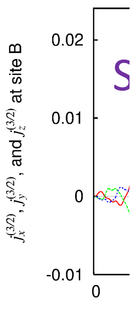

$$l_x = \begin{pmatrix} 0 & 0 & 0 \\ 0 & 0 & -i \\ 0 & i & 0 \end{pmatrix},\quad l_y = \begin{pmatrix} 0 & 0 & i \\ 0 & 0 & 0 \\ -i & 0 & 0 \end{pmatrix},\quad l_z = \begin{pmatrix} 0 & -i & 0 \\ i & 0 & 0 \\ 0 & 0 & 0 \end{pmatrix}$$

Strong field case

High-freq. expansion in Floquet theory: $H_F^{(2)}$

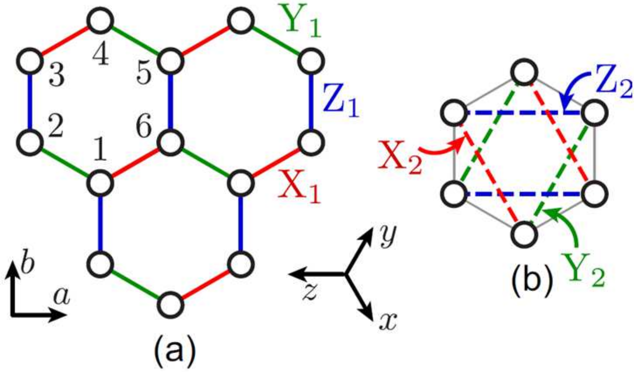

$$H_F^{(2)} = \sum_{m>0} \frac{[H_m, H_{-m}]}{m\hbar\omega}$$

For left-hand circular polarization and at site A,

$$H_F^{(2,A)} = \sum_{m>0} \frac{1}{m\hbar\omega} \sum_{kab\sigma} J_m^2\left(\frac{eaF_L}{\hbar\omega}\right)(2i)\sin\frac{2m\pi}{3}(\star)_{ab} c^\dagger_{\boldsymbol{k},a,\sigma} c_{\boldsymbol{k},b,\sigma}$$

At site B, momenta are reversed.

where

$$\star = e^{i\boldsymbol{k}\cdot X_2}T_1^Y T_1^Z - e^{-i\boldsymbol{k}\cdot X_2}T_1^Z T_1^Y + e^{i\boldsymbol{k}\cdot Y_2}T_1^Z T_1^X - e^{-i\boldsymbol{k}\cdot Y_2}T_1^X T_1^Z + e^{i\boldsymbol{k}\cdot Z_2}T_1^X T_1^Y - e^{-i\boldsymbol{k}\cdot Z_2}T_1^Y T_1^X$$

$$= [T_1^Y, T_1^Z]\cos\boldsymbol{k}\cdot X_2 + [T_1^Z, T_1^X]\cos\boldsymbol{k}\cdot Y_2 + [T_1^X, T_1^Y]\cos\boldsymbol{k}\cdot Z_2$$

$$+ i\{T_1^Y, T_1^Z\}\sin\boldsymbol{k}\cdot X_2 + i\{T_1^Z, T_1^X\}\sin\boldsymbol{k}\cdot Y_2 + i\{T_1^X, T_1^Y\}\sin\boldsymbol{k}\cdot Z_2$$

- Single-orbital systems have only ***k***-odd terms with anticommutators.
- Multi-orbital systems have ***k***-even terms with commutators, in addition.

$$H_F^{(2)} \simeq \frac{1}{\hbar\omega}\sum_{iab\sigma} J_1^2\left(\frac{eaF_L}{\hbar\omega}\right)(2i)\sin\frac{2\pi}{3}\left([T_1^Y, T_1^Z] + [T_1^Z, T_1^X] + [T_1^X, T_1^Y]\right)_{ab} c^\dagger_{i,a,\sigma} c_{i,b,\sigma}$$

$$\simeq \underline{\frac{1}{\hbar\omega}J_1^2\left(\frac{eaF_L}{\hbar\omega}\right)\sqrt{3}(t_2 - t_4)[t_2 - t_4 + 2(t_3 - t_1)]} < 0 \text{ for L(, > 0 for R)}$$

$$\times \sum_{i\sigma}\begin{pmatrix} c^\dagger_{i,yz,\sigma} & c^\dagger_{i,xz,\sigma} & c^\dagger_{i,xy,\sigma} \end{pmatrix}\begin{pmatrix} 0 & -i & i \\ i & 0 & -i \\ -i & i & 0 \end{pmatrix}\begin{pmatrix} c_{i,yz,\sigma} \\ c_{i,xz,\sigma} \\ c_{i,xy,\sigma} \end{pmatrix}$$

Emergence of angular momentum in multi-orbital systems

- Left-hand circular pol.

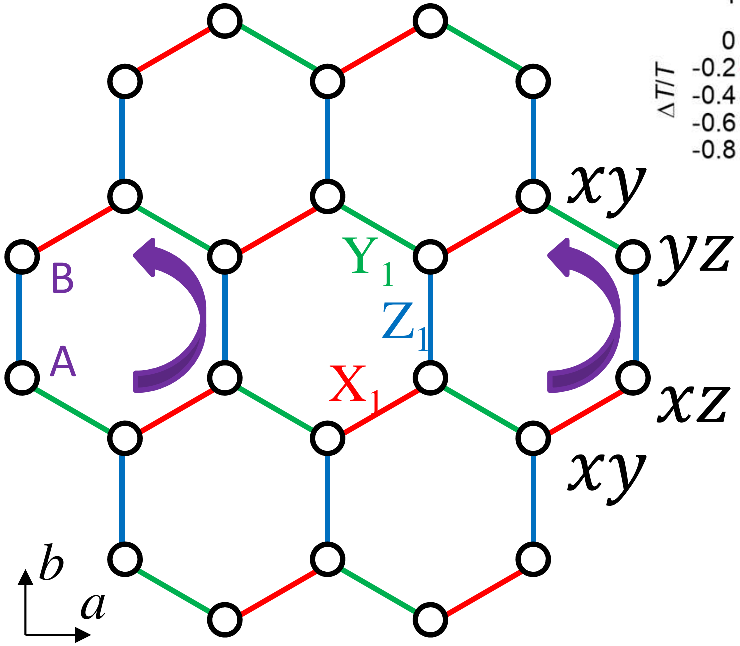

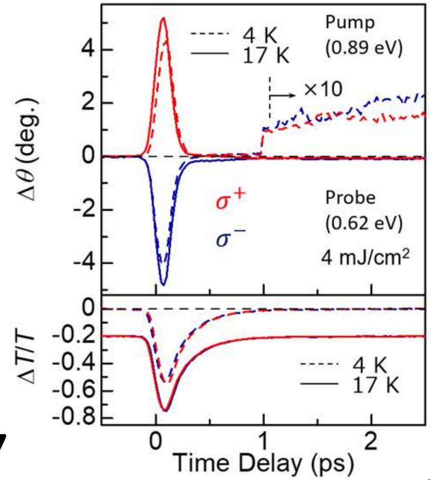

T. Amano, KY, S. Iwai *et al.*
Phys. Rev. Res. (2022).

- Right-hand circular pol.

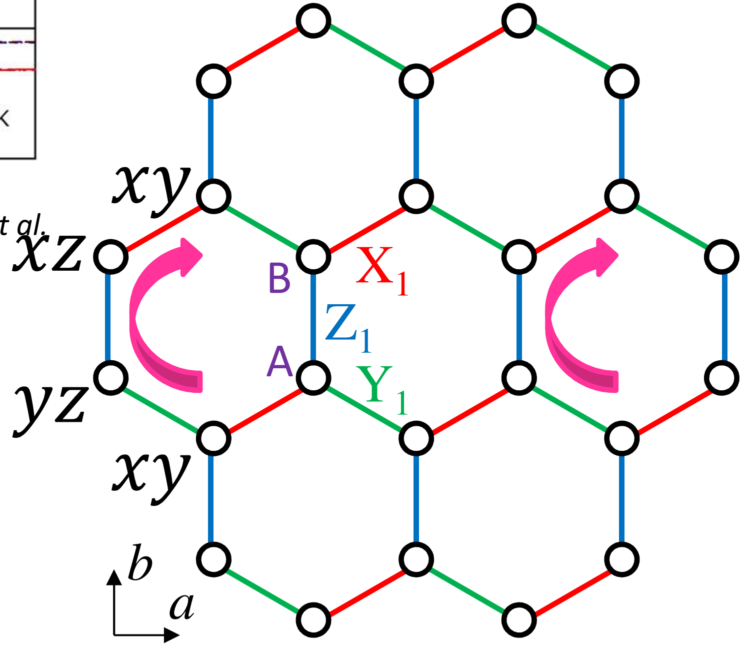

- Main transitions when (interorbital) t_2 processes are dominant.
- Quantitatively, (intraorbital) t_3 processes are also important.

$$\mathbf{T}_1^Z = \begin{pmatrix} t_1 & t_2 & t_4 \\ t_2 & t_1 & t_4 \\ t_4 & t_4 & t_3 \end{pmatrix}$$

Summary on effective mag. fields in multi-orb. systems

- Photoinduced magnetization in α-$RuCl_3$: explained by Floquet theory.
- $H_F^{(2)} = \sum_{m>0} \frac{[H_m, H_{-m}]}{m\hbar\omega}$ gives a helicity-dependent effective magnetic field on $l_{\text{eff}} \perp$ honeycomb plane.
- $H_{F,\text{SO}}^{(3)} \equiv \sum_{m\neq 0} \frac{[H_{-m},[H_{\text{SO}},H_m]]}{2(m\hbar\omega)^2}$ gives rotating effective magnetic fields on l_{eff} & s ∥ honeycomb plane, which are antiparallel between A & B.

Intersite interorbital hopping processes are essential.

Charge DOF in frustrating spin systems for emergent magnetization

in the spin-orbit assisted Mott insulator.

⇔ effective magnetic fields deep in the insulating phase.

A. Sriram and M. Claassen, arXiv 2021, S. Banerjee et al., PRB 2022

Summary

- Now, many-electron states can be manipulated in various manners.
- Synchronized charge oscillation
  - Transient charge order
  - Stimulated emission
  - SHG in centrosymmetric systems (Space-inversion symmetry breaking)
- Effective magnetic fields in multi-orbital systems
  - Emergence of magnetization ⊥ lattice
  - Inverse Faraday effect
  - Time-reversal symmetry breaking